POLITECNICO DI TORINO
Repository ISTITUZIONALE

Leaky-wave Analysis and Design of a Corrugated Sectoral Waveguide

(Article begins on next page)

22 December 2024

Leaky-wave Analysis and Design
of a Corrugated Sectoral Waveguide

Matteo Perrone*, Julien Sarrazin† ‡, Guido Valerio† ‡, Guido Lombardi*

* Department of Electronics and Telecommunications (DET), Politecnico di Torino, 10129, Turin, Italy
{matteo_perrone, guido.lombardi}@polito.it
† Sorbonne Université, CNRS, Laboratoire GeePs, 75252, Paris, France
‡ Université Paris-Saclay, CentraleSupélec, CNRS, Laboratoire GeePs, 91192, Gif-sur-Yvette
{julien.sarrazin, guido.valerio}@sorbonne-universite.fr

Abstract—A dispersive analysis of a fully metal corrugated sectoral waveguide is presented. This structure supports cylindrical mode and closed-form solutions are not available in literature due to the presence of the corrugations. The phase constant of the cylindrical mode is extracted by means of a full-wave calculation of the fields excited with a rectangular-waveguide feed. The sectoral waveguide is periodic modulated introducing concentric circular slots. Thus a periodic leaky-wave antenna is obtained. The radiated patterns validate the phase constant computed in the waveguide without slots.

Index Terms—periodic leaky-wave antenna, corrugations, radial waveguide.

I. INTRODUCTION

2D leaky-wave antennas (LWAs) based on a sectoral horn waveguide, i.e., a radial waveguide with a rectangular flange input, have been successfully designed to achieve high-gain [1]. Engineering the frequency dispersion of the leaky wave (i.e. its phase and attenuation constants) is of utmost importance to tailor LWA radiation. For instance, [2], [3] use corrugations inside rectangular waveguides in order to increase the leaky dispersion, thereby the frequency-beam-scanning of LWAs, whereas [4] uses pins.

Unfortunately, closed-form formulas are not available in the literature to calculate dispersion diagrams using such type of periodic loadings inside radial waveguides, see Figs. 1. Furthermore, a circular geometry does not allow for classical periodic dispersive analysis based on a single unit cell in Cartesian coordinates with commercial software.

To estimate the wavenumber inside a sectoral horn waveguide with periodic corrugations in the lower plate, full-wave simulations of the finite structure are conducted in this paper. From the electric-field distribution, the guided-wavelength is obtained from which the wavenumber is inferred. Section II assesses this approach with a sectoral horn waveguide with no corrugations for which closed-form expression of the phase constant exists. Section III uses this approach to investigate the influence of the corrugations on the dispersion diagram. A periodic LWA is designed in section IV where the relationship

between its radiation and its phase constant is observed. Finally, section V draws some conclusions.

II. SECTORAL WAVEGUIDE ANALYSIS

The sectoral waveguide under consideration is shown in Fig. 1(a). It consists in a wedge waveguide fed by a rectangular waveguide. In a cylindrical coordinate system (ρ, ϕ, z), the structure has a wedge-plate geometry with horizontal plates at $z = 0, b$ and vertical plates at $\phi = 0, \phi_0$, where $\phi_0 = 72.7°$ is the aperture angle. Along the ρ direction, the antenna side length is equal to $L = 131.50$ mm. The positions of the front and rear faces are at ρ_0 and $(L + \rho_0)$. The value of ρ_0 is 4.8 mm. The feeding is a rectangular-waveguide port of width $a = 7.112$ mm and height $b = 3.556$ mm (WR28 standard).

The geometry in Fig. 1(a) corresponds to the sectoral horn waveguide described in [5]. The following wave functions can be used to describe a field inside the structure with a closed-form expression:

$$\psi_{mp}^{\text{TM}}(\rho, \phi, z) = \cos\left(\frac{m\pi}{a}z\right) \sin\left(\frac{p\pi}{\phi_0}\phi\right) H_{p\pi/\phi_0}^{(2)}(k_\rho\rho) \quad (1)$$

where $H_{p\pi/\phi_0}^{(2)}$ is the Hankel function of second kind of order $p\pi/\phi_0$ and $k_\rho = \sqrt{k_0^2 - (m\pi/a)^2}$. The scenario in this paper considers a single TM^z mode propagation within the frequency range of interest, with no field variation along the waveguide height, i.e., $m = 0$ and $p = 1$, so $k_\rho = k_0$. By using asymptotic formulas for Hankel functions, for large values of the real argument $k_\rho\rho$, the radial oscillations of the field approach a periodic, which allow to define a spatial period of the field at a given time instant, guided-wavelength λ_g as the guided-wavelength in the sectoral waveguide, related to $k_\rho = \beta$ as $k_\rho = \beta = 2\pi/\lambda_g$.

We propose here a simple procedure to compute the wavenumber k_ρ from this relation. This method is not necessary in the structure without corrugations, but it becomes useful when the corrugations are present since a simple closed-form expression for k_ρ is no more available. The k_ρ is named here β since it is the phase constant of the radial wave and, even if perturbed by the slots, of the leaky wave in the open structure studied in the next section.
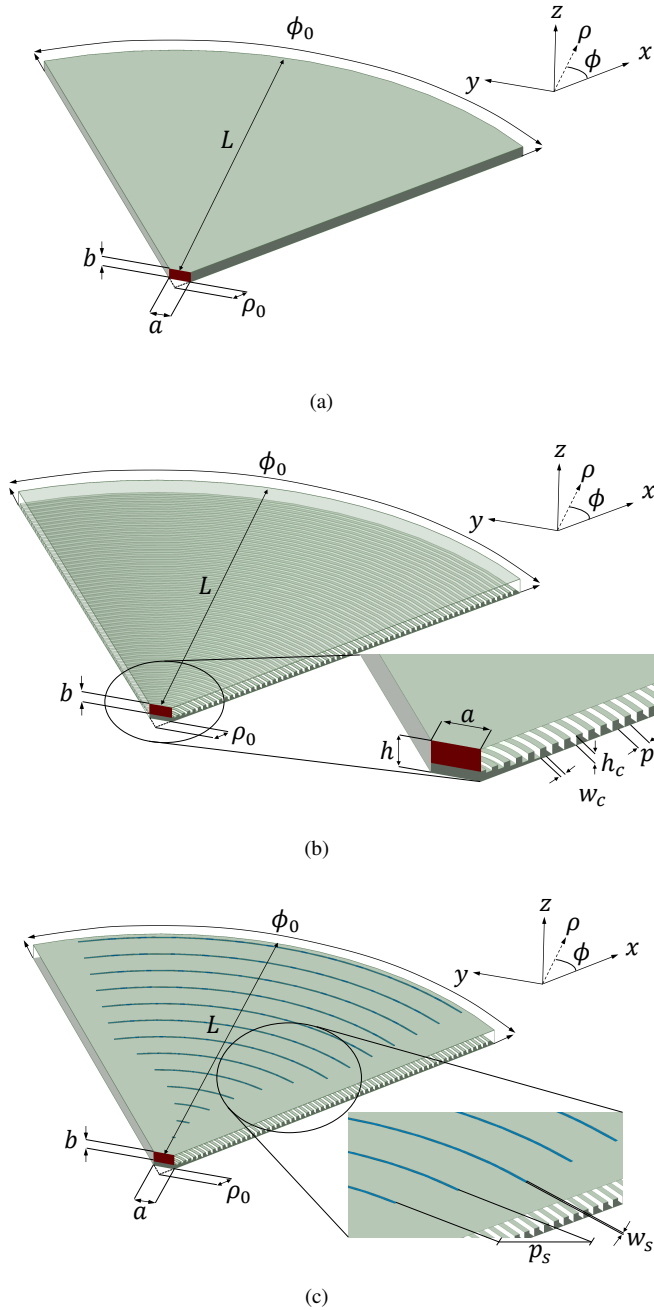
Fig. 1. Sectoral waveguides studied in this paper. The structure has a wedge-plate geometry with horizontal and vertical plates at $z = 0, b$ and $\phi = 0, \phi_0$, respectively. The ϕ_0 is the aperture angle of the sectoral waveguide. The side of the waveguide along ρ direction is L. The positions of the front and rear faces are at ρ_0 and $(L + \rho_0)$, respectively. Each sector is fed with a rectangular waveguide port, in red, of dimensions a and b. (a) Sectoral waveguide with PEC on lateral, bottom and up plates. (b) Sectoral waveguide with corrugated bottom plate. The height h along z direction is $h_c + b$, where h_c is the height of corrugations. The period and the width of the corrugations are p_c and w_c, respectively. A smooth tapering of the corrugation depths is done. (c) Sectoral waveguide with circular slots and corrugated bottom plate. The period and the width of the slots are p_s and w_s, respectively. A initial tapering of the first six slots is done.($\phi_0 = 72.7°$, $L = 131.50$ mm, $\rho_0 = 4.8$ mm, $a = 7.112$ mm, $b = 3.556$ mm, $h_c = 1.575$ mm, $p_c = 2$ mm, $w_c = 1$ mm, $p_s = 9.934$ mm, $w_s = 0.54$ mm).

The wavelength λ_g is estimated inside the structure by computing the spatial distance between adjacent zeros of the z component of the electric field E_z, computed with full-wave simulations (using Ansys HFSS). We compared the results extracting from HFSS with those of the closed form ψ_{01}^{TM} in (1) along a line in ρ direction at $\phi = \phi_0/2$ and $z = b/2$. The outward-only propagation in Ansys HFSS is ensured by adding an absorbing condition right at the end of the sectoral waveguide. Therefore, across the antenna radial distance, the guided-wavelength is not exactly constant, an averaging procedure is used on the field extracted from full-wave simulations to estimate the phase constant.

Across the frequency range of interest, i.e., 26.5-29 GHz, there are between 10 and 11 spatial periods of E_z along the antenna radial length. By averaging those lengths of those periods to reduce numerical errors in field computation, a single guided-wavelength is retained per frequency point. It is to be noted that the first spatial period, i.e., the closest to the feeding port, is discarded from the average calculation not to take into account any effects due to the feeding port proximity. The dispersion obtained is shown in Fig. 2. The β_{HFSS} and β_ψ are the phase constants obtained with the guided-wavelength estimated from the full-wave simulations and (1), respectively. Since $m = 0$, k_ρ is here equal to the free-space wavenumber k_0. It is observed that the phase constant estimated from HFSS electric field and from the closed-form wave function expression are very close to each other. The slight discrepancy may be due to the presence of the waveguide port which could excite several radial waves in its vicinity. Both β_{HFSS} and β_ψ are close to, but less than, k_ρ. This is expected as only for large $k_\rho\rho$ does the Hankel function approaches a periodic function. These results give some confidence about the estimation of the phase constant using the full-wave electric field. In the next section, the same procedure is therefore applied to the corrugated structure, for which no closed-form field expression is available in the literature. The corrugations parameters are chosen so that the surface is equivalent to a homogeneous reactance.
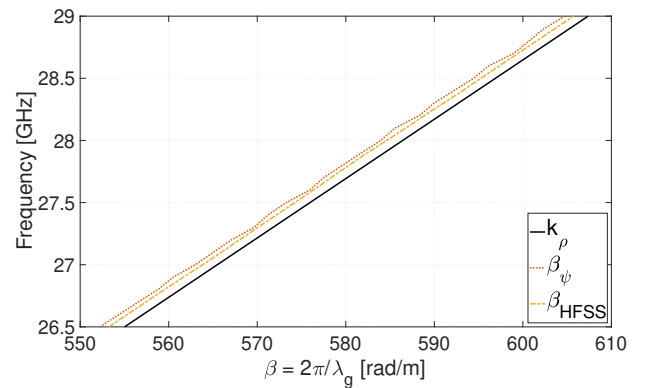

Fig. 2. Dispersion diagram of the sectoral waveguide in Fig. 1(a). Comparison between k_ρ in (1) (equal here to the free-space wavenumber k_0) and the dispersions obtained by averaging the guided-wavelength estimated from HFSS-extracted field β_{HFSS} and from closed-form wave function β_ψ.

III. Corrugated Sectoral Waveguide

Extending the procedure of [2] oriented to rectangular waveguide geometries, concentric circular corrugations are built in the lower plate of the radial waveguide. A smooth tapering of the corrugation depth is done to avoid impedance mismatch. The period and the width of the corrugations are $p_c = 2\,\mathrm{mm}$ and $w_c = 1\,\mathrm{mm}$, respectively, as shown in Fig. 1(b). Each corrugation can be treated as a shorted transmission line. The objective is to increase β, thus reducing the guided wavelength λ_g of the propagating mode being $\lambda_g = 2\pi/\beta$ [6], [7]. Within the range of values considered, higher depths of corrugation correspond to an increasing of β. Since a higher β will reach in a shorter bandwidth the endfire from the broadside, the LWA can scan faster in the presence of the corrugations.

Using the procedure presented in the previous section, the dispersion diagrams for the three corrugation depths $h_c = [1.375, 1.475, 1.575]\,\mathrm{mm}$ are calculated and shown in Fig. 3. As expected, corrugations slow down the wave propagation and lead to a faster β-frequency variation, which in turns induces faster frequency-beam-scanning velocity in LWA.

of concentric circular slots, the structure can be regarded as a locally periodic slotted waveguide. The local direction of periodicity being the radial direction. In this way fast space harmonics can be generated from the slow-wave range obtained with $h_c = 1.575\,\mathrm{mm}$ in order to achieve a leaky-wave radiation. The slotted periodic LWA is shown in Fig 1(c). The space-harmonic phase constants are given by:

$$\beta_n = \beta + \frac{2n\pi}{p_s}, \qquad n = 0, \pm 1, \pm 2, ... \tag{2}$$

where β is the phase constant inside the non-modulated sectoral waveguide, i.e., as calculated in the previous section, and p_s is the distance between the periodic slots, assuming the slots do not strongly modify the fundamental mode of the closed waveguide. By choosing $p_s = 9.934\,\mathrm{mm}$, the dispersion diagram shown in Fig. 4 is obtained. The -1 space harmonic is fast across the whole 26.5-29 GHz frequency range, as well as the -2 space harmonic after 27.25 GHz. This choice is done simply as a benchmark to assess whether the methodology followed in this paper estimates the phase constant in such a way that the LWA beam direction is correctly described by the well-known formula [8]:
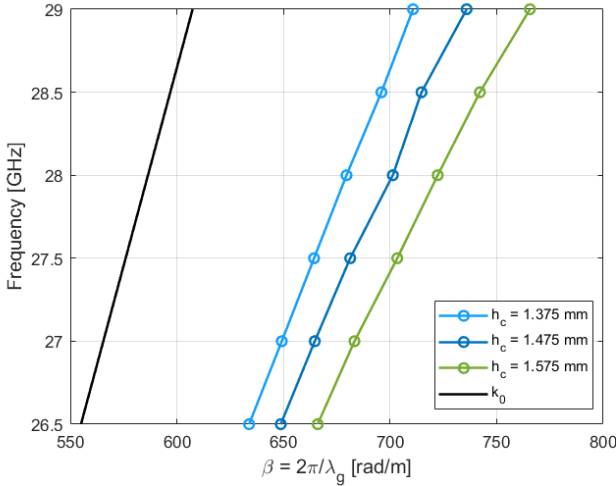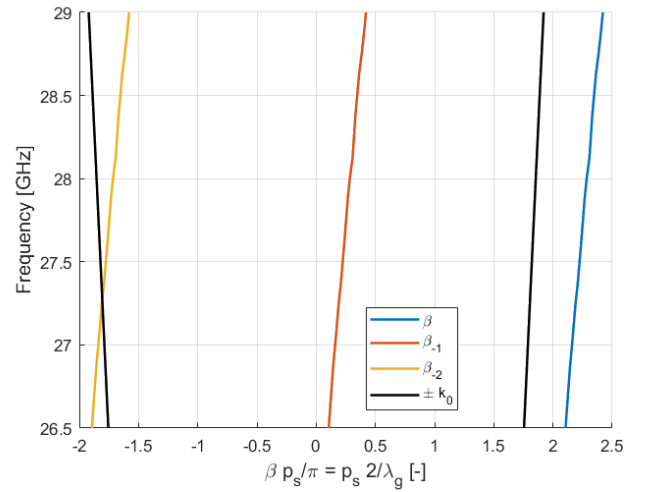
$$\theta_n = \sin^{-1} \beta_n / k_0 \tag{3}$$

Fig. 3. Dispersion diagram of the sectoral waveguide in Fig. 1(b) with different heights of corrugations (h_c), i.e. $h_c = [1.375, 1.475, 1.575]\,\mathrm{mm}$. Line of light is reported, i.e. k_0. The corrugations are placed on the lower plate. A variation of h_c implies a changing of the phase constant β. For higher values we can see a shift of the dispersion curve far from the line of light k_0. Higher corrugation depth implies an increase of frequency-beam-scanning velocity. The depth chosen for the following structures is $h_c = 1.575\,\mathrm{mm}$.

Fig. 4. Dispersion diagram of the locally periodic sectoral structure in Fig. 1(c). Period of the slots chosen is $p_s = 9.934\,\mathrm{mm}$. Two beams are visible, the first β_{-1} at whole band in analysis: $f = [26.5, 29]$ GHz, the second approximately at $f = [27.25, 29]$ GHz. Lines of lights are reported, i.e. $\beta = \pm k_0$.

IV. Leaky-Wave Antenna

As we can see in the dispersion diagram of Fig. 3 for $h_c = 1.575\,\mathrm{mm}$, $\beta > k_0$, therefore the dominant mode is in the slow-wave range. Some periodic modulation need to be introduced in the guiding structure to make it radiate. Periodic slots produce an infinity of space harmonics, some of which may be fast, and therefore radiate [8].

By modulating the upper plate of the structure with a series

The slots have a circular shape, concentric with the waveguide geometry. The slots width are set to $w_s = 0.54\,\mathrm{mm}$, which is about $\lambda_0/20$, where λ_0 is the free space wavelength at the central frequency of 27.75 GHz. The length of the first six slots is tapered in order to achieve a smooth transition between the waveguide input and the slotted section. The 13 slots are etched along the antenna radial length, whose dimensions are given in Table I. The LWA reflection coefficient is shown in Fig. 5. Except in the higher part of the frequency band, the

slot #	l_s [mm]
1	1.05
2	4.40
3	12.20
4	23.50
5	38.25
6	56.50
7	78.20
8	88.50
9	98.95
10	109.80
11	119.80
12	130.20
13	140.60

Fig. 6. Realized gain of the corrugated leaky-wave antenna. The frequency beam scanning is notable for the -1 and -2 space harmonics in the $[0, 20°]$ and $[-90°, -50°]$ angular ranges, respectively.
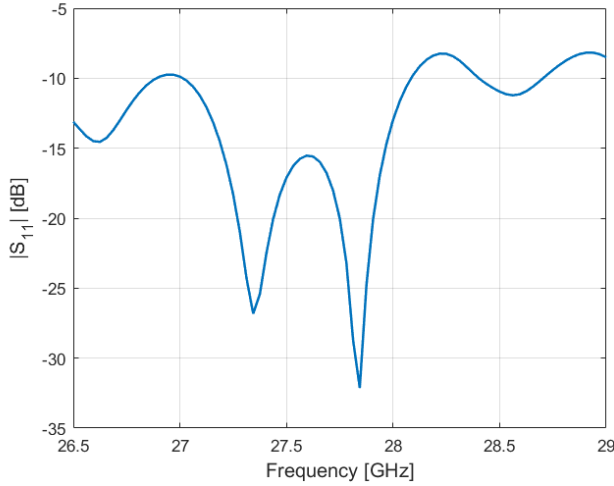

Fig. 5. Simulated reflection coefficient of the corrugated leaky-wave antenna in Fig. 1(c). The antenna is well matched with a reflection coefficient below $-10\,$dB, apart from the higher frequency band.

Fig. 7. Comparison of the beam direction obtained by full-wave simulations. In solid line using theoretical formula (3) and in solid line with circle markers directly by commercial solver (Ansys HFSS). A good agreement is visible.

antenna is well matched with a reflection coefficient below -10 dB. The realized gain as a function of θ angle is shown in Fig. 6. The frequency-beam-scanning is noticeable for the -1 space harmonic in the $[0, 20°]$ angular range, and for the -2 harmonic within $[-90°, -50°]$.

The beam direction obtained by full-wave simulations (in Ansys HFSS) and those obtained by (3) are shown in Fig. 7. The agreement of these directions confirm the correctness of the calculation of the dispersion diagram as explained in the previous sections. These results open the way to a design of the slot distribution based on the properties of the closed waveguide in order to meet the desired features of the radiation pattern and maximizing the rapidity of scan of the structure.

V. CONCLUSIONS

We have applied a method to estimate the phase constant of radial modes propagating in sectoral corrugated waveg-
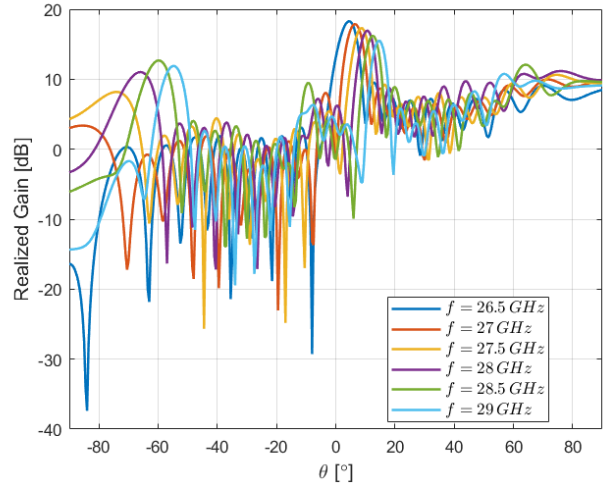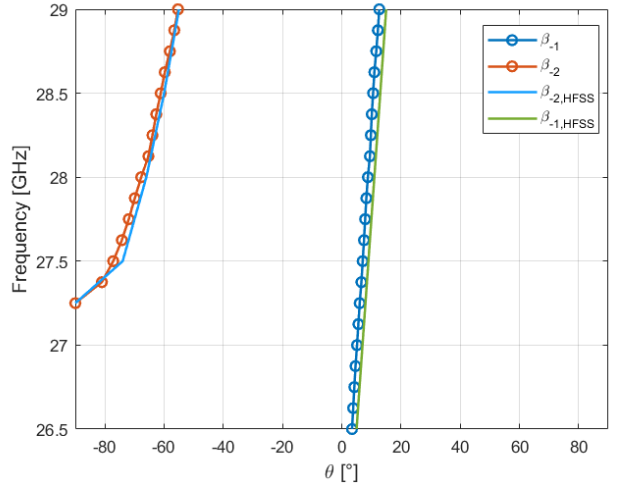
uides. The corrugations allow to enhance the frequency-beam-scanning velocity of the LWA once a periodic set of slots is opened on the top metal plate of the structure. The results are validated by comparing the theoretical leaky results and the simulated radiation patterns. The method will be extended for the computation and the optimization of the leaky attenuation constant, and will therefore allow for the design of periodic sectoral LWA providing desired radiation features.

REFERENCES

[1] A. Attar, A. R. Sebak, "High gain periodic 2-D leaky-wave antenna with backward radiation for millimeter-wave band", in *IEEE Open J. Antennas Propag.*, vol. 2, pp. 49-61, 2021, doi: 10.1109/OJAP.2020.3043634.
[2] J. Sarrazin, G. Valerio, "H-plane-scanning multibeam leaky-wave antenna for wide-angular-range AoA estimation at mm-wave", *17th Eu-*

ropean Conference on Antennas and Propagation (EuCAP), Mar. 2023, Florence, Italy.

[3] Z. Liu, *et Al.*, "Compact fully metallic millimeter-wave waveguide-fed periodic leaky-wave antenna based on corrugated parallel-plate waveguides," in *IEEE Antennas Wireless Propag. Letters*, vol. 19, no. 5, pp. 806-810, May 2020, doi: 10.1109/LAWP.2020.2980993.

[4] J. Chen, *et Al.*, "Linearly sweeping leaky-wave antenna with high scanning rate," in *IEEE Trans. Antennas Propag.*, vol. 69, no. 6, pp. 3214-3223, Jun. 2021, doi: 10.1109/TAP.2020.3037830.

[5] R. F. Harrington, "Cylindrical wave functions" in *Time-harmonic electromagnetic fields*, Wiley-IEEE Press, 2001, ch. 5.

[6] C. Balanis, "Rectangular cross-section waveguides and cavities" in *Advanced engineering electromagnetics*, 2nd ed., Wiley, 2012, ch. 8.

[7] R. E. Collin, "Periodic structure and filters" in *Foundations of microwave engineering*, 2nd ed., Wiley, 2001, ch. 8.

[8] A. A. Oliner, "Leaky-wave antennas" in *Antenna engineering handbook*, R. C. Johnson, 3rd ed., McGraw-Hill, 1992, ch. 10.